

Mixing and Power Consumption of Structured Fluids in Stirred Reactors

Giuseppina Montante^{a,*}, Gianluca Boccardo^b, Nicola Antonio Di Spirito^c, Nino Grizzuti^c, Francesco Maluta^a, Daniele Marchisio^b, Alessandro Paglianti^a, Rossana Pasquino^c

^aDepartment of Industrial Chemistry, Università di Bologna, via Piero Gobetti 85, 40129, Bologna, Italy

^bDepartment of Applied Science and Technology, Politecnico di Torino, C.so Duca degli Abruzzi 24, 10129 Torino, Italy

^cDepartment of Chemical, Materials and Industrial Production Engineering, Università degli Studi di Napoli Federico II, P.le Tecchio 80, 80125 Napoli, Italy
giuseppina.montante@dunibo.it

This work deals with the fluid dynamics characterization of structured fluids, which are adopted in the preparation and processing of many products in different industrial applications. Experiments on binary mixtures of water and Pluronic L64 are carried out in a laboratory stirred reactor, by varying the mixture concentrations and the temperature, thus obtaining different microstructures of Pluronic molecules in water corresponding to different fluid rheology. The fluid dynamics characteristics are measured by Stereo Particle Image Velocimetry. The resulting data are presented and discussed with the final purpose of providing insight into the prevailing flow regimes, the velocity field and the shear rate in the reactor volume. In addition, power consumption measured by a strain gauge system allows to estimate the energy requirement expected in the industrial operations. The results show significant spatial variations of the velocity field and related variables. The data can be adopted for the improvement of the design and operation of the reactors and for the validation of a multiscale modelling methodology of the same systems.

1. Introduction

The local fluid dynamics characterization of stirred tanks for complex fluids processing has been carried out in a relatively small number of investigations with respect to the case of turbulent Newtonian fluids (Simon et al., 2024). It can provide significant insight into the rheological behaviour during the fluid preparation, the determination of the local apparent viscosity and consequently the improvement of modelling methods of stirred reactors, where significant spatial variations are expected and either the transitional flow regime or variable regimes depending on the location inside the same vessel can take place (Gabelle et al., 2013).

In this work the case of Pluronic in water is considered, due to the industrial interest of this specific class of synthetic copolymers, which are characterized by a wide versatility. They are obtained from the sequential polymerization of monomers of propylene oxide and ethylene oxide, leading to triblock copolymers made up of a central hydrophobic chain of poly-propylene oxide and two lateral hydrophilic blocks of poly-ethylene oxide. The self-assembling of Pluronics in solution gives rise to many different morphologies depending on temperature and composition. Details on the specific Pluronic investigated in this work, that is the L64, including the binary phase diagram in water, has been recently presented in the review of Di Spirito et al. (2024), where an overview on Pluronics with a focus on their properties and phase transition behaviour can be found.

Multiscale modelling methods, such as those recently proposed by De Roma et al. (2024), combining the rheology model obtained from dissipative particle dynamics simulation with the Computational Fluid Dynamics simulation of a static mixer, can take advantage from multiscale experimental investigations for improving model robustness and for validation.

In the following, the results obtained in a stirred tank with Pluronic L64 in water at different concentrations and temperatures in selected cases are presented and discussed.

2. Material and Methods

The investigation was carried out in an unbaffled reactor made of Perspex, that is shown in Figure 1 together with the schematic view of the instrumentation for the Stereoscopic Particle Image Velocimetry (SPIV) and the torque measurements. The tank, of diameter, T , equal to 230 mm and height, H_T , equal to 290 mm, was stirred by a Rushton turbine of diameter D equal to 76.7 mm placed at the impeller clearance, C , of 101 mm from the bottom of the cylindrical part of the vessel. The stirred tank was filled with 10 L of Pluronic L64 water solutions at different concentrations. The temperature was measured at the beginning and at the end of each run and the maximum increase due to agitation was of 0.1 °C. For the flow field measurements, the impeller speed, N , was fixed at 350 rpm for avoiding surface aeration from the central vortex, which forms with the less viscous fluids. Correspondingly, the impeller tip speed, V_{tip} , was equal to 1.41 m/s. For the torque measurements, the impeller speed was varied.

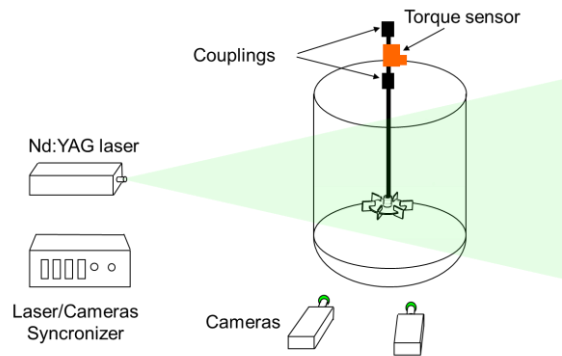


Figure 1: Sketch of the stirred tank with the schematic view of the SPIV and torque measurement instrumentation

The rotational Reynolds number, Re , considered for data discussion, is defined as:

$$Re = \frac{\rho N D^2}{\mu} \quad (1)$$

In case of non-Newtonian rheology, following Metzner and Otto, the apparent viscosity is calculated, assuming that the shear rate is proportional to the impeller speed with the constant of proportionality equal to 11, as recommended for fast impellers. The investigated liquid compositions and temperatures and the relevant physical properties are summarized in Table 1, where T_f is the fluid temperature, ρ is the density, μ the viscosity and $\dot{\gamma}$ the shear rate.

Table 1: Water-Pluronic L64 mixtures and investigated conditions

Pluronic wt. %	T_f (°C)	Phase	ρ (kg/m ³)	μ (Pa·s)
30	25	Micellar	1015	0.015
50	25	Micellar	1025	0.65
50	30	Hexagonal	1025	$76.3\dot{\gamma}^{0.41}$

2.1 Stereo Particle Image Velocimetry

The instantaneous velocity field was measured by a Dantec Dynamics SPIV system. It consisted of a Nd:YAG Litron DualPower laser, emitting light at wavelength of 532 nm with energy of 50 mJ per pulse, and two SpeedSense Lab 340 cameras of resolution of 2,560 × 1,600 pixel each fixed on a Scheimpflug mount. One of the cameras was set perpendicularly to the laser light sheet, while the other was at an angle of 20° with respect to the first one. The laser light sheet, approximately 2 mm thick, entered the vessel vertically on a diametrical plane. To minimize optical distortion of the laser light, the vessel was placed within a larger square vessel made of Perspex filled with water, being the refractive index of water and of the water-Pluronic mixtures very similar. The flow was seeded with silver-coated hollow glass particles of mean diameter equal to 10 μm and density of 1,100 kg/m³, resulting in a particle relaxation time in the range 10⁻⁸-10⁻⁶ s. The instantaneous velocity vectors were obtained by acquiring 2,000 double frame images at the rate of 5 Hz and at time interval between two laser pulses, Δt , determined experimentally with the same criteria usually adopted for PIV measurements in unbaffled vessels (Montante and Paglianti, 2015). The raw image pairs were analyzed individually by an adaptive-correlation algorithm implemented in the DynamicStudio software, with interrogation areas of initial size equal

to 64 x 64 pixel and final size of 16 x 16 pixel, resulting in a velocity field spatial resolution of 1.56 mm. The peak heights in the correlation plane and the velocity magnitude were selected for the instantaneous vector validation. The ensemble averaged mean and fluctuating velocities on the planar measurement section were obtained by combining the two-dimensional instantaneous vector fields using a calibration model. At higher Re, statistical convergence of the mean velocity was obtained with 500 valid instantaneous vectors. Instead, at least 1,500 instantaneous vectors were required to ensure statistical convergence of the fluctuating velocity. This value lowered at decreasing Reynolds number. The average measurement uncertainties can be obtained considering the uncertainty in the PIV measurements of 2-3 % of the velocity vector, the additional uncertainties of 0.07-0.4 pixel for the SPIV and 2-3 times larger uncertainties for the out-of-plane displacement components (Sciacchitano et al., 2019).

2.2 SPIV data post-processing

The data discussion is based on the analysis of the mean and the fluctuating components of the fluid velocity and their gradients. The three velocity components were determined in a cartesian coordinate system with the origin placed on the center of the impeller disk, assuming the x coordinate positive if directed toward the vessel wall, the y coordinate positive if directed upwards and the z coordinate positive if opposite to the impeller rotation direction. In this coordinate system, U, V, W are the mean velocity components and u', v', w' are the root mean square (rms) velocity fluctuations in the x, y, z direction respectively. It is worth observing that, being the measurement performed in a vertical diametrical plane, x coincides with the radial coordinate, y with the axial coordinate and z with the tangential coordinate.

The mean velocity, U, is calculated as the ensemble average of the instantaneous velocity values, u(t), as:

$$U = \frac{\sum_{i=1}^{N_{cv}} u_i(t)}{N_{cv}} \quad (2)$$

where N_{cv} is the number of validated instantaneous velocities.

The velocity fluctuation, u', is calculated as the square root of the variance, that represents the deviation of the instantaneous velocity from the mean velocity, as:

$$u' = \sqrt{\frac{\sum_{i=1}^{N_{cv}} (u_i(t) - U)^2}{N_{cv}}} \quad (3)$$

Being the double-frame images collected at variable impeller blade position, the velocity fluctuations include the so-called pseudo-turbulence.

The shear rate, $\dot{\gamma}$, is calculated with different approximations on the tangential gradients, which cannot be measured by SPIV. Considering the shear rate definition:

$$\dot{\gamma} = \sqrt{2 \left(\left(\frac{du}{dx} \right)^2 + \left(\frac{dv}{dy} \right)^2 + \left(\frac{dw}{dz} \right)^2 \right) + \left(\frac{du}{dy} + \frac{dv}{dx} \right)^2 + \left(\frac{du}{dz} + \frac{dw}{dx} \right)^2 + \left(\frac{dv}{dz} + \frac{dw}{dy} \right)^2} \quad (4)$$

the tangential gradients of the tangential velocity are obtained from the continuity equation for incompressible fluids. Instead, the tangential gradients of the axial and radial velocity cannot be included. As a result, the approximate value of the shear rate is computed as:

$$\dot{\gamma} = \sqrt{2 \left(\left(\frac{du}{dx} \right)^2 + \left(\frac{dv}{dy} \right)^2 + \left(\frac{dw}{dz} \right)^2 \right) + \left(\frac{du}{dy} + \frac{du}{dx} \right)^2 + \left(\frac{dw}{dx} \right)^2 + \left(\frac{dw}{dy} \right)^2} \quad (5)$$

The shear rate obtained neglecting the tangential velocity gradients is also calculated for comparison with the case of planar PIV measurements.

2.3 Torque

The energy consumption of the mixing operation was obtained by measuring the torque on the shaft using the Kistler torque sensor type 4501, which is based on a strain gauges system, maximum measurable torque of 2 Nm and accuracy class of 0.2. The sensor was mounted between the motor and the bearing assembly. The power transferred by the shaft to the fluid through the impeller was calculated as the torque times the impeller speed. For each rotational speed, the torque due to friction dissipation with the rotating shaft in the empty vessel was subtracted to the measured power. Dynamic measurements were performed starting from completely separated phases (water on top of pure Pluronic), from the onset of agitation, that was instantaneously switched

on at the selected impeller speed, to the complete homogenization of the two phases. Afterwards, the power consumption was obtained for all the fluids listed in Table 1 at variable impeller speeds at the steady state.

3. Results and discussion

The effect of concentration and temperature on the macroscopic fluid properties, that is related to Pluronic self-assembling behaviour, can be appreciated in Figure 2a. The fluid viscosity is constant with the shear rate for both mixtures at 25 °C, while a pseudo-plastic behaviour is obtained at 50 wt. % of Pluronic L64 at 30 °C.

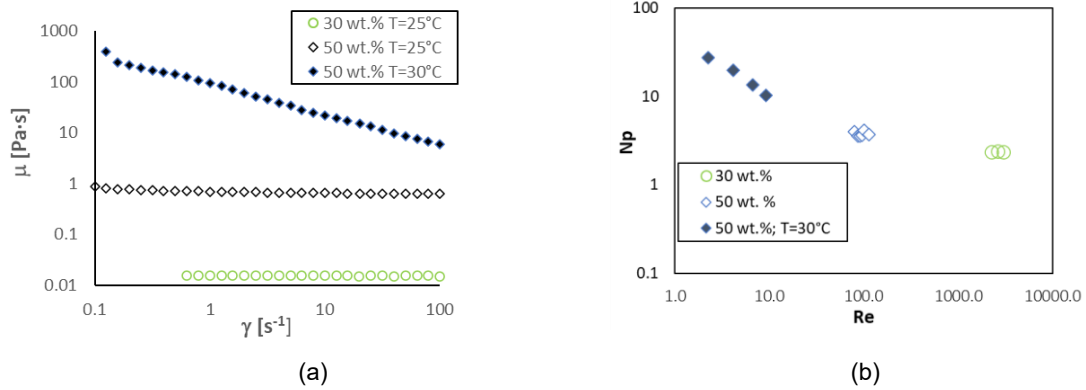


Figure 2: Flow curves (a) and power curves (b) of the water-Pluronic mixtures for different concentrations and temperatures.

The trend of the power number for the three mixtures stirred at different impeller speeds corresponding to different rotational Reynolds numbers in Figure 2b suggests that the flow is laminar up to $Re=10$, while at higher Re the flow is in the transitional regime. It is also worth reporting that the time trace of the power consumption measured from the onset of agitation starting from completely separated phases measured in selected conditions revealed that the achievement of the steady state conditions takes a very long time. For instance, the transient curve, which is not shown for the sake of space, lasts about 1 h and the power requirement is up to 25 % higher than the value required at the steady state for the preparation of the 50 wt. % mixture at ambient temperature.

The magnitude of the three velocity components of the 30 and the 50 wt.% mixtures in the vertical diametrical section close to the impeller are shown in Figure 3 and Figure 4, respectively. In general, the fluid is mainly driven in the tangential direction, since the tangential velocity is more marked than the other two components, the axial recirculation is strongly dependent on the fluid composition and the radial component is significant just in the impeller discharge stream in both cases.

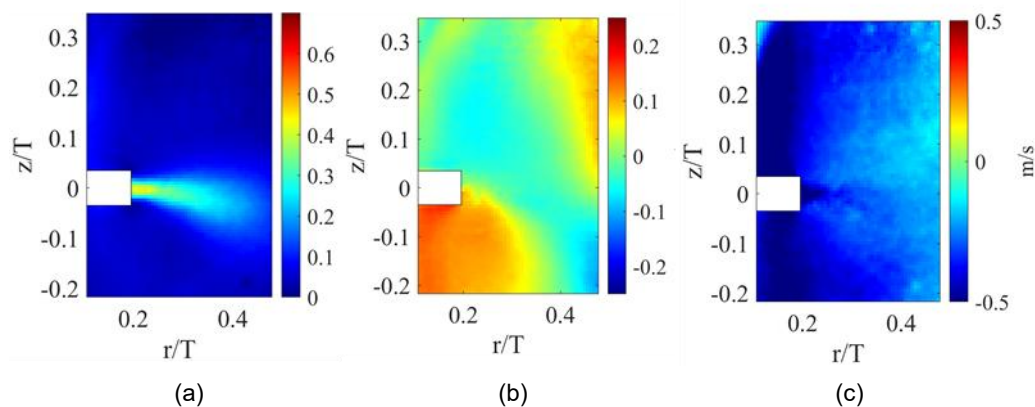


Figure 3: Radial (a), axial (b) and tangential (c) velocity magnitude in a diametrical vertical plane for the 30 wt.% mixture at 25 °C stirred at 350 rpm.

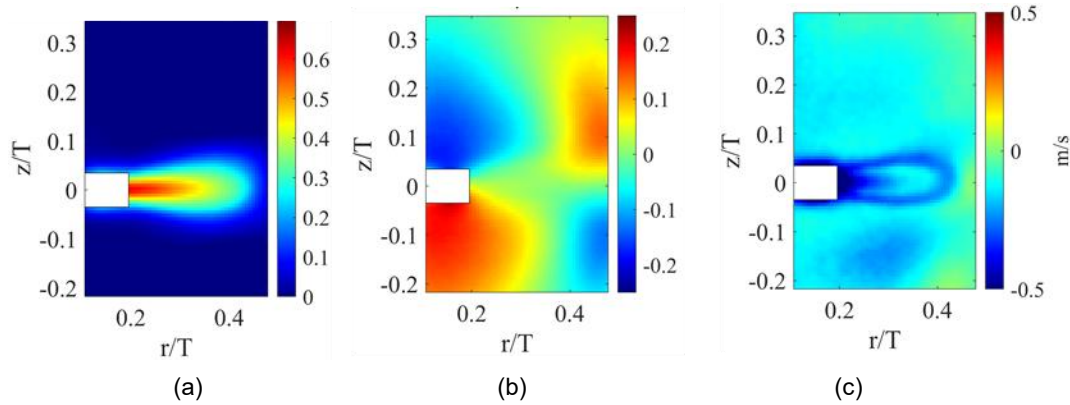


Figure 4: Radial (a), axial (b) and tangential(c) velocity magnitude in a diametrical vertical plane for the 50 wt. % mixture at 25 °C stirred at 350 rpm.

The velocity fluctuations shown in Figure 5 and 6 are negligible in the radial and axial component, apart very close to the impeller, particularly for the more dilute mixture. The higher values of the tangential fluctuations can be mainly due to pseudo-turbulence.

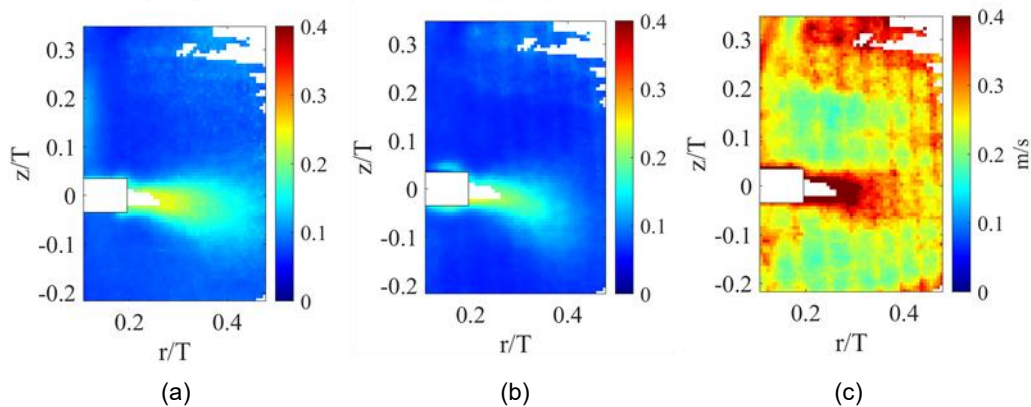


Figure 5: Radial (a), axial (b) and tangential (c) velocity fluctuations in a diametrical vertical plane for the 30 wt. % mixture at 25 °C stirred at 350 rpm. In the white zones, data are not depicted due the low number of valid instantaneous velocities.

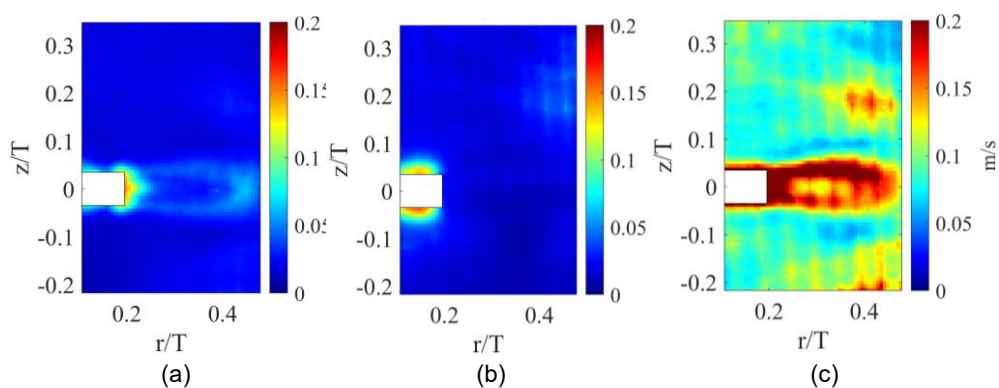


Figure 6: Radial (a), axial (b) and tangential (c) velocity fluctuations in a diametrical vertical plane for the 50 wt. % mixture at 25 °C stirred at 350 rpm.

It is worth pointing out that the ensemble averaged data are often collected under turbulent conditions (Delafosse et al., 2011), since the removal of the periodic component does not significantly affect the calculation of the turbulence quantities, while in the investigated system, further insight in the flow characteristics moving from laminar to transitional flow regime would require angle resolved data.

The shear rate map obtained from the instantaneous velocity data with Eq(5) for the 30 wt.% mixture shown in Figure 7a confirm that due to the significant heterogeneity in the stirred tank the adoption of a single average value for the whole vessel is not appropriate (Gabelle et al., 2013) and the importance to account for the three dimensionality of the flow is apparent considering the results obtained neglecting the tangential component, shown in Figure 7b.

The data can be further exploited to perform a comparison of different statistical methods for the determination the local apparent viscosity (Simon et al., 2024). Also they can be compared with the results of Computational Fluid Dynamics (CFD) modelling methods, which are particularly challenging to devise in the case of non-Newtonian transitional regimes for the scale-up of industrial equipment.

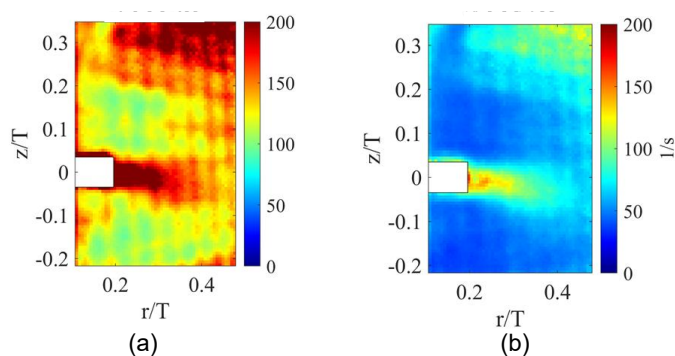


Figure 7: Shear rate including (a) and excluding the tangential velocity component (b) for the 30 wt. % mixture at 25 °C stirred at 350 rpm.

4. Conclusions

Water-Pluronic L64 mixtures are investigated considering pure laminar to transitional flow in a stirred tank, which are confirmed by the power curve trend. Significant spatial variations of mean and fluctuating velocities are obtained depending on the composition and temperature of the fluids. Stereo and Planar PIV results provide significantly different shear rates, due to the important contribution of the tangential velocity component. Based on the flow characteristics, useful guidelines for the spatial discretization of computational domain in CFD calculations can be obtained. Overall, the experimental results provide information on the interplay between the reactor geometrical characteristics and the fluids rheology and their effect on the hydrodynamics for appropriate modelling aimed at improving reactors scale-up.

Acknowledgments

This study was carried out within the “Non-equilibrium self-assembly of structured fluids: a multiscale engineering problem” project funded by European Union–Next Generation EU within the PRIN 2022 program (D.D. 104 - 02/02/2022 Ministero dell'Università e della Ricerca).

References

- Delafosse, A., Collignon, M.-L., Crine, M., Toye, D., 2011, Estimation of the turbulent kinetic energy dissipation rate from 2D-PIV measurements in a vessel stirred by an axial Mixel TTP impeller, *Chemical Engineering Science*, 66,, 1728-1737.
- De Roma F., Marchisio D., Boccardo G., Bouaifi M., Buffo A., 2024, Application of a multiscale approach for modeling the rheology of complex fluids in industrial mixing equipment, *Physics of Fluids*, 36, art. no. 023119.
- Di Spirito, N.A., Grizzuti, N., Pasquino, R., 2024, Self-assembly of Pluronics: A critical review and relevant applications, *Physics of Fluids*, 36, art. no. 111302.
- Gabelle J.-C., Morchain J., Anne-Archard D., Augier F., Liné A., 2013, Experimental determination of the shear rate in a stirred tank with a non-newtonian fluid: Carbopol, *AIChE Journal*, 59, 2251 - 2266
- Montante G., Paglianti A., 2015, Fluid dynamics characterization of a stirred model bio-methanation digester, *Chemical Engineering Research and Design*, 93, 38 – 47.
- Sciacchitano, A., 2019, Uncertainty quantification in particle image velocimetry, *Measurement Science and Technology*, 30, art. no. 092001.
- Simon E., Augier F., Morchain J., Pierson J.-L., Liné A., 2024, Investigation of the local apparent viscosity in a stirred tank with a shear-thinning fluid through particle image velocimetry, *Chemical Engineering Research and Design*, 206, 378 – 385.